

Table VII. Reduction Potentials for Fe<sup>III</sup>/Fe<sup>II</sup> Couples

compd	pot., V	ref. pot.	pot. vs NHE <sup>28</sup>	ref
Fe(enterobactin)	-1.23	SCE	-0.99	29
FeO <sub>2</sub> <sup>-</sup>	-0.68	NHE	-0.68	30
Fe <sub>2</sub> O[HB(pz) <sub>3</sub> ] <sub>2</sub> <sup>-</sup> (OAc) <sub>2</sub>	-0.76	SCE	-0.52	31
Fe(Pctad)ClO <sub>4</sub>	-0.945	Ag/Ag <sup>+</sup>	-0.400	33
Fe(Saltad)ClO <sub>4</sub>	-0.79	Ag/Ag <sup>+</sup>	-0.25	33
Fe(Mesaldpt)Cl	-0.66	Ag/Ag <sup>+</sup>	-0.12	33
Fe(TPP)Cl	-0.29	SCE	-0.05	34
Fe(py-pentaamine) <sup>2+</sup>	-0.27	SCE	-0.03	35
Fe(EDTA) <sup>-</sup>	0.12	NHE	0.12	36
Fe([16]aneN <sub>5</sub> )	-0.04	SCE	0.20	36
Fe(ibz)Cl <sub>3</sub>	-0.4	Fc <sup>+</sup> /Fc	0.30	32
Fe[(TPP)Br <sub>4</sub> ]	0.083	Ag/AgCl	0.305	38
Fe(tacn) <sub>2</sub>	0.13	Ag/AgCl	0.35	37
Fe[TPP(CN) <sub>3</sub> ]	0.185	Ag/AgCl	0.407	38
Fe(dtne)Br <sub>3</sub>	0.41	NHE	0.41	39
Fe[TPP(CN) <sub>4</sub> ]	0.215	Ag/AgCl	0.438	38
Fe[HB(pz) <sub>3</sub> ] <sub>2</sub> <sup>+</sup>	0.23	SCE	0.47	31
Fe(CN) <sub>6</sub> <sup>3-</sup>	0.55	NHE	0.55	36
Fc <sup>+</sup>	0.34	SCE	0.58	40
Fc—C≡C—Fc	0.46, 0.60	SSCE	0.70, 0.84	41
Fe <sup>3+</sup> (aq)	0.77	NHE	0.77	42
Fe(bpy) <sub>3</sub> <sup>3+</sup>	0.82	SCE	1.06	43
Fe(tppb) <sub>2</sub>	0.855	SSCE	1.091	this work
Fe(phen) <sub>3</sub> <sup>3+</sup>	1.14	NHE	1.14	30
Fe(Me <sub>2</sub> bpy) <sub>3</sub> <sup>3+</sup>	0.912	SCE	1.154	44
Fe(NO <sub>2</sub> phen) <sub>3</sub> <sup>3+</sup>	1.25	NHE	1.25	30

temperature and undergoes a spin crossover at 393 K, Fe[HB(3,5-Me<sub>2</sub>pz)<sub>3</sub>]<sub>2</sub>, with longer Fe–N bond lengths, was found to be high-spin at room temperature.<sup>11</sup> Thus, it is not surprising that Fe(tppb)<sub>2</sub>, with still longer Fe–N bonds, is a high-spin complex at room temperature. Similar conversion of a spin-crossover Fe(II)

system to a high-spin Fe(II) complex has been observed previously.<sup>45</sup>

## Conclusions

Despite expectations to the contrary, a phenyl group substituent in the 3-position of the pyrazole ring in the hydrotris(pyrazol-1-yl)borate ligand is not sufficiently bulky to prevent formation of the bis complex in the absence of a strongly coordinating ligand such as SCN<sup>-</sup>. In the context of non-heme oxygenase modeling this is disappointing, as one would prefer to maintain open coordination sites for binding of substrate and/or dioxygen. On the other hand, we have observed a greater reactivity of **1** and **2** toward O atom donors such as PhIO and MCPBA as compared to their less hindered counterparts, presumably indicating that removal of one of the bulky ligands is feasible. This is not surprising on the basis of the marked increase in Fe–N bond lengths for **1** compared to Fe[HB(pz)<sub>3</sub>]<sub>2</sub>. In addition to providing a more reactive metal center, the bulky ligand causes large shifts in the redox potentials for both Fe<sup>III</sup>/Fe<sup>II</sup> and Mn<sup>III</sup>/Mn<sup>II</sup> couples. Further investigations into the reactivities of **1** and **2**, particularly under oxidizing conditions, are underway.

**Acknowledgment.** Support for this work was provided by Grant No. GM382751-01 from the National Institutes of General Medical Sciences. We thank Dr. Frederick J. Hollander and Dr. Marilyn M. Olmstead for assistance with the crystal structure determinations.

**Registry No.** **1**, 128576-17-0; **2**, 128576-18-1; Ktpbb, 106209-98-7; Fe[HB(pz)<sub>3</sub>]<sub>2</sub><sup>+</sup>, 86549-95-3; KBH<sub>4</sub>, 13762-51-1; 3-phenylpyrazole, 2458-26-6.

**Supplementary Material Available:** For both **1** and **2**, tables of positional and isotropic equivalent thermal parameters, anisotropic thermal parameters, intramolecular distances, and intramolecular angles (21 pages); listings of structure factors for **1** and **2** (57 pages). Ordering information is given on any current masthead page.

(45) Harris, C. R.; Patil, H. R. H.; Sinn, E. *Inorg. Chem.* **1969**, *8*, 101.

## Notes

Contribution from the Department of Chemistry, University of Wyoming, Laramie, Wyoming 82071

### Calcium Binding to Carboxylate Residues: Synthesis and Structure of a New Form of Calcium Malonate

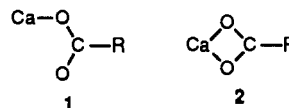
Derek J. Hodgson\* and R. Owen Asplund

Received February 14, 1990

There has been intense recent interest in the modes of binding of the calcium ion to carboxylate and (especially) dicarboxylate moieties because of the significance of such interactions in the blood and bone proteins that contain the modified amino acid residues  $\gamma$ -carboxyglutamic acid (Gla) and  $\beta$ -carboxyaspartic acid (Asa).<sup>1-5</sup> It is well established that Gla residues are implicated in the binding of calcium ions in both blood and bone proteins,<sup>6</sup> and several authors have suggested that a principal role for Gla might be in the discrimination between calcium and magnesium ions.<sup>7</sup> Consequently, we and others have been investigating the

structural properties of a series of model complexes that are designed to permit the evaluation of the possible modes of binding of calcium, magnesium, and related metals to Gla and/or Asa.<sup>8-11</sup>

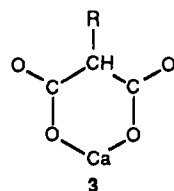
The binding of calcium ions to carboxylates has been discussed exhaustively by Einspahr and Bugg;<sup>12</sup> these authors note that a monocarboxylate (e.g. Glu or Asp) can bind to calcium in either of two ways. In a unidentate mode (**1**) the metal binds to a single oxygen atom, while in a bidentate fashion (**2**) the metal binds to



both oxygen atoms of the carboxylate group. In a dicarboxylate (e.g. Gla or Asa) there is an additional possible mode in which the metal ion binds to two oxygen atoms from different carboxylate groups; this mode of binding, which is sometimes referred to as the "malonate" mode since it is uniquely available to a dicarboxylate like malonate, is shown in **3**.

- Magnusson, S.; Sottrup-Jensen, L.; Peterson, T. E.; Morris, H. R.; Dell, A. *FEBS Lett.* **1974**, *44*, 189-193.
- Stenflo, J.; Fernlund, P.; Egan, W.; Roepstorff, P. *Proc. Natl. Acad. Sci. U.S.A.* **1974**, *71*, 2730-2733.
- Prendergast, F. G.; Mann, K. G. *J. Biol. Chem.* **1977**, *252*, 840-850.
- Lian, J. B.; Hauschka, P. V.; Gallop, P. M. *Fed. Proc.* **1978**, *37*, 2615-2620.
- Christy, M. R.; Barkley, R. M.; Koch, T. H.; Van Buskirk, J. J.; Kirsch, W. M. *J. Am. Chem. Soc.* **1981**, *103*, 3935-3937; Christy, M. R.; Koch, T. H. *J. Am. Chem. Soc.* **1982**, *104*, 1771-1772.
- Jackson, C. M.; Nemerson, Y. *Annu. Rev. Biochem.* **1980**, *49*, 765-811.

- Williams, R. J. In *Calcium Binding Proteins and Calcium Function*; Wasserman, R. H., et al., Eds.; Elsevier: New York, 1977; pp 1-12.
- Zell, A.; Einspahr, H.; Bugg, C. E. *Biochemistry* **1985**, *24*, 533-537.
- Curry, M. E.; Eggleston, D. S.; Hodgson, D. J. *J. Am. Chem. Soc.* **1985**, *107*, 8234-8238; Curry, M. E.; Hodgson, D. J.; Eggleston, D. S. *Rev. Port. Quim.* **1985**, *27*, 344.
- Yokomori, Y.; Hodgson, D. J. *Inorg. Chem.* **1988**, *27*, 2008-2011.
- Yokomori, Y.; Flaherty, K. A.; Hodgson, D. J. *Inorg. Chem.* **1988**, *27*, 2300-2306.
- Einspahr, H.; Bugg, C. E. *Acta Crystallogr., Sect. B* **1981**, *B37*, 1044-1052.



While no definitive structural study of a metal complex of Gla or Asa has appeared, several workers have modeled these residues by the use of malonate or of  $\alpha$ -substituted malonate ions.<sup>8-11</sup> Of particular significance to the present study are the reports of the binding of calcium to ethylmalonate,<sup>8</sup> methylmalonate,<sup>9</sup> and benzylmalonate<sup>10</sup> ions. In addition, two hydrated forms of calcium malonate have been studied; in the form of (malonato)diaquacalcium(II),  $[\text{Ca}(\text{mal})(\text{OH}_2)_2]$ , grown from aqueous solution, the malonate ions are involved in interactions of types 1 and 2 but not of type 3<sup>13-15</sup> while in the gel form only types 1 and 3 are observed.<sup>16</sup> We have now isolated a third form of this complex in which the complex crystallizes as a dihydrate, i.e. as  $[\text{Ca}(\text{mal})(\text{OH}_2)_2] \cdot 2\text{H}_2\text{O}$ . We here report the synthesis and structural properties of this new form of (malonato)diaquacalcium(II).

### Experimental Section

**Synthesis.** Malonic acid (10.4 g, 0.1 mol) was dissolved in 250 mL of membrane-purified, deionized water. The solution was set in agitation, and calcium oxide was added in approximately 100-mg quantities. After each addition, the solution was allowed to become clear before the subsequent addition of further CaO; the time required for this clarification increased with each addition. The addition of CaO was continued until slight cloudiness persisted for several hours, which occurred at a calcium ion to malonic acid ratio of very nearly 1:2, and the pH of the solution was 3.0. The solution was filtered through paper and the clear filtrate allowed to evaporate slowly in a hood. Crystallization typically began after about 8 days, and recovered crystals were air-dried and combined. The total yield, based on the calcium added, was 85%. The colorless prismatic crystals were recrystallized from water as above. Anal. Calc for  $\text{Ca}_3\text{H}_{10}\text{O}_8$ : Ca, 18.71; C, 16.82; H, 4.71. Found (mean of four different preparations): Ca,  $18.2 \pm 0.4$ ; C,  $17.0 \pm 0.3$ ; H,  $4.7 \pm 0.2$ . Calcium carbonate may be used in place of calcium oxide to give a resultant product that is indistinguishable from that obtained with CaO.

**X-ray Crystallography.** Intensity data were collected on a Nicolet R3m/V diffractometer equipped with a molybdenum tube [ $\lambda(\text{K}\alpha_1) = 0.70926 \text{ \AA}$ ;  $\lambda(\text{K}\alpha_2) = 0.71354 \text{ \AA}$ ]. Data were corrected for Lorentz-polarization effects and for absorption. Additional details concerning the data collection and reduction are presented in Table I.

The structure was solved by direct methods and refined by full-matrix least-squares techniques. All hydrogen atoms were refined isotropically, while other atoms were refined anisotropically. The final atomic positional parameters are presented in Table II; lists of thermal parameters and observed and calculated structure amplitudes are available as supplementary material.

### Discussion

The structure consists of  $[\text{Ca}(\text{mal})(\text{H}_2\text{O})_2]$  molecules, which are hydrogen bonded to lattice water molecules. As is invariably found for calcium complexes of malonate and its derivatives, the structure is polymeric.<sup>8-10,13-16</sup> A view of the coordination around a single calcium ion is shown in Figure 1, and the inner coordination sphere is depicted in Figure 2. The significant bond lengths and angles in the complex are collected in Tables III and IV, respectively.

As is seen in Figures 1 and 2, the calcium ions are eight-coordinate in the complex, the coordination sites being occupied by six malonate oxygen atoms and the two water molecules. Examination of Figure 2 clearly demonstrates that the geometry at calcium is well described as a square antiprism, although the deviations from the idealized interplanar angles<sup>17</sup> are severe as

Table I. Crystallographic and Data Collection Parameters

formula	$\text{Ca}_3\text{H}_{10}\text{O}_8$	$T, ^\circ\text{C}$	22
$a, \text{ \AA}$	10.601 (2)	$D_0, \text{ g cm}^{-3}$	1.77 (3)
$b, \text{ \AA}$	6.7217 (13)	$Z$	4
$c, \text{ \AA}$	12.347 (3)	$D_c$	1.749
$\beta, \text{ deg}$	112.412 (14)	space group	$P2_1/c$
$V, \text{ \AA}^3$	813.4 (3)	$\mu, \text{ mm}^{-1}$	0.76
NO	2460	data range	$4 < 2\theta < 60^\circ$
NO(obs)	1802 [ $I > 3\sigma(I)$ ]	data collected	$\pm h, \pm k, \pm l$
radiation	Mo $\text{K}\alpha$	$R$	0.0256
		$R_w$	0.035

Table II. Atomic Coordinates ( $\times 10^4$ ) for  $[\text{Ca}(\text{mal})(\text{OH}_2)_2] \cdot 2\text{H}_2\text{O}$

atom	X	Y	Z
Ca(1)	4191 (1)	1329 (1)	1799 (1)
O(1)	6277 (1)	2053 (1)	1419 (1)
O(2)	6606 (1)	5320 (1)	1630 (1)
O(3)	5784 (1)	2058 (1)	-1340 (1)
O(4)	6191 (1)	5217 (1)	-1510 (1)
C(1)	6718 (1)	3686 (1)	1201 (1)
C(2)	7447 (1)	3648 (2)	336 (1)
C(3)	6412 (1)	3643 (1)	-921 (1)
O(5W)	3384 (1)	1356 (1)	-290 (1)
O(6W)	1647 (1)	1453 (2)	1042 (1)
O(7W)	10044 (1)	3554 (2)	3633 (1)
O(8W)	8753 (1)	-55 (2)	2896 (1)
H(1C2)	7980 (17)	2456 (26)	477 (15)
H(2C2)	8063 (17)	4823 (24)	504 (14)
H(1W5)	3425 (20)	2287 (20)	-686 (18)
H(2W5)	3610 (20)	412 (31)	-542 (17)
H(1W6)	1200 (21)	559 (34)	1242 (17)
H(2W6)	1320 (23)	1369 (27)	316 (21)
H(1W7)	10394 (30)	3960 (40)	3152 (24)
H(2W7)	9756 (22)	2406 (39)	3467 (21)
H(1W8)	8743 (24)	-1019 (36)	3368 (22)
H(2W8)	7886 (26)	428 (36)	2512 (18)

Table III. Bond Lengths ( $\text{ \AA}$ ) for  $[\text{Ca}(\text{mal})(\text{OH}_2)_2] \cdot 2\text{H}_2\text{O}^a$

Ca(1)-O(1)	2.478 (1)	Ca(1)-O(5W)	2.389 (1)
Ca(1)-O(6W)	2.496 (1)	Ca(1)-O(2C)	2.487 (1)
Ca(1)-O(3A)	2.349 (1)	Ca(1)-O(3B)	2.519 (1)
Ca(1)-O(4D)	2.361 (1)	Ca(1)-O(4B)	2.561 (1)
O(1)-C(1)	1.261 (1)	O(2)-C(1)	1.244 (1)
O(3)-C(3)	1.259 (1)	O(4)-C(3)	1.254 (1)
C(1)-C(2)	1.539 (2)	C(2)-C(3)	1.522 (1)

<sup>a</sup> Symmetry operations: (A)  $1 - x, -y, -z$ ; (B)  $x, 1/2 - y, 1/2 + z$ ; (C)  $1 - x, -1/2 + y, 1/2 - z$ ; (D)  $1 - z, 1 - y, -z$ .

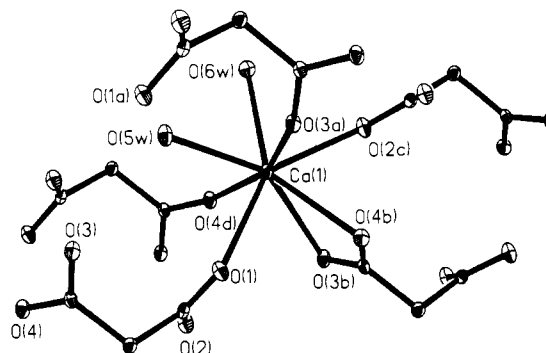


Figure 1. View of the coordination around a single calcium(II) ion in the crystals of  $[\text{Ca}(\text{mal})(\text{OH}_2)_2] \cdot 2\text{H}_2\text{O}$ , showing the five different malonate dianions and two water molecules to which the calcium ion is bonded. Symmetry operations are as in Table III.

a result of the constraints due to the bidentate nature of the binding to O(3b) and O(4b). Eight-coordinate calcium ions are also found in the solution-grown crystals of  $[\text{Ca}(\text{mal})(\text{OH}_2)_2]^{13-15}$  but not in the gel phase;<sup>16</sup> eight-coordinate calcium ions are also found in

(13) Briggman, B.; Oskarsson, Å. *Acta Crystallogr., Sect. B* 1977, B33, 1900-1906.

(14) Karipides, A.; Ault, J.; Reed, A. T. *Inorg. Chem.* 1977, 16, 3299-3302.

(15) Marsh, R. E.; Schomaker, V. *Inorg. Chem.* 1979, 18, 2331-2336.

(16) Albertsson, J.; Oskarsson, Å.; Svensson, C. *Acta Crystallogr., Sect. B* 1978, B34, 2737-2743.

(17) Muettertiess, E. L.; Guggenberger, L. J. *J. Am. Chem. Soc.* 1974, 96, 1748-1756.

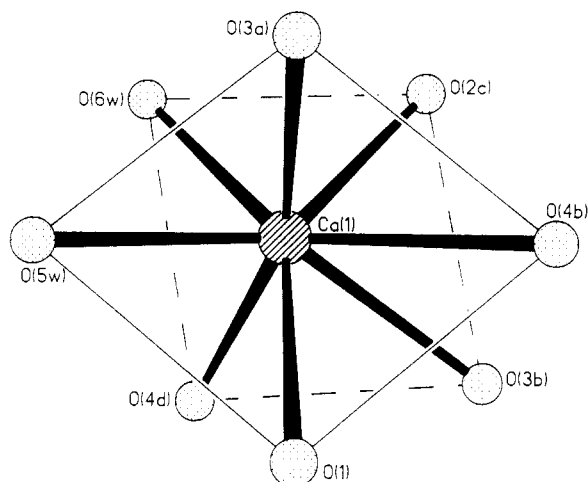


**Figure 2.** View of the inner coordination sphere around a single calcium(II) ion in the crystals of  $[\text{Ca}(\text{mal})(\text{OH}_2)_2] \cdot 2\text{H}_2\text{O}$ , showing the distorted square-antiprismatic geometry at calcium. Symmetry operations are as in Table III.

**Table IV.** Bond Angles (deg) for  $[\text{Ca}(\text{mal})(\text{OH}_2)_2] \cdot 2\text{H}_2\text{O}^a$

O(1)–Ca(1)–O(5W)	76.8 (1)	O(1)–Ca(1)–O(6W)	146.8 (1)
O(5W)–Ca(1)–O(6W)	72.8 (1)	O(1)–Ca(1)–O(2C)	142.6 (1)
O(5W)–Ca(1)–O(2C)	139.1 (1)	O(6W)–Ca(1)–O(2C)	70.2 (1)
O(1)–Ca(1)–O(3A)	92.9 (1)	O(5W)–Ca(1)–O(3A)	77.2 (1)
O(6W)–Ca(1)–O(3A)	93.0 (1)	O(2A)–Ca(1)–O(3A)	87.9 (1)
O(1)–Ca(1)–O(3B)	75.6 (1)	O(5W)–Ca(1)–O(3B)	145.2 (1)
O(6W)–Ca(1)–O(3B)	125.4 (1)	O(2A)–Ca(1)–O(3B)	73.5 (1)
O(3A)–Ca(1)–O(3B)	124.9 (1)	O(1)–Ca(1)–O(4D)	83.8 (1)
O(5W)–Ca(1)–O(4D)	81.9 (1)	O(6W)–Ca(1)–O(4D)	79.2 (1)
O(2C)–Ca(1)–O(4D)	107.3 (1)	O(3A)–Ca(1)–O(4D)	159.0 (1)
O(3B)–Ca(1)–O(4D)	74.4 (1)	O(1)–Ca(1)–O(4B)	73.3 (1)
O(5W)–Ca(1)–O(4B)	136.7 (1)	O(6W)–Ca(1)–O(4B)	139.4 (1)
O(2C)–Ca(1)–O(4B)	71.1 (1)	O(3A)–Ca(1)–O(4B)	73.8 (1)
O(3B)–Ca(1)–O(4B)	51.1 (1)	O(4D)–Ca(1)–O(4B)	124.3 (1)
Ca(1)–O(1)–C(1)	129.9 (1)	C(1)–O(2)–Ca(1b)	133.5 (1)
C(3)–O(3)–Ca(1d)	150.1 (1)	C(3)–O(3)–Ca(1c)	94.4 (1)
Ca(1d)–O(3)–Ca(1c)	105.2 (1)	C(3)–O(4)–Ca(1a)	154.3 (1)
C(3)–O(4)–Ca(1c)	92.5 (1)	Ca(1a)–O(4)–Ca(1c)	103.6 (1)
O(1)–C(1)–O(2)	125.0 (1)	O(1)–C(1)–C(2)	117.3 (1)
O(2)–C(1)–C(2)	117.7 (1)	C(1)–C(2)–C(3)	110.5 (1)
O(3)–C(3)–O(4)	121.6 (1)	O(3)–C(3)–C(2)	119.0 (1)
O(4)–C(3)–C(2)	119.5 (1)		

<sup>a</sup>Symmetry operations: (A)  $1 - x, -y, -z$ ; (B)  $x, 1/2 - y, 1/2 + z$ ; (C)  $1 - x, -1/2 + y, 1/2 - z$ ; (D)  $1 - x, 1 - y, -z$ ; (a) = D; (b)  $1 - x, 1/2 + y, 1/2 - z$ ; (c)  $x, 1/2 - y, -1/2 + z$ ; (d) = A.

one of the two independent ions of calcium methylmalonate.<sup>9</sup>

As can be seen in Figure 1, each calcium ion binds to five different malonate groups, forming four unidentate interactions (1) and one bidentate (2) interaction; there are no examples of malonate interactions (3) in the structure. Hence, the binding here is slightly reminiscent of that in one form of calcium methylmalonate.<sup>9</sup> The modes of binding observed in the various calcium complexes of malonate and substituted malonate ions are compared in Table V. As can be seen from an examination of that table, the calcium ions in these complexes show remarkable coordinative flexibility.

The Ca–O bond lengths in the structure are in the range 2.349 (1)–2.561 (1) Å. As expected, the Ca–O bonds in the bidentate mode are longer than those in the unidentate interactions. The bidentate bond lengths of 2.519 (1) and 2.561 (1) Å [average 2.54 (3) Å] are in excellent agreement with the average of 2.53 (7) Å observed in other bidentate calcium carboxylates.<sup>12</sup> The four unidentate carboxylate interactions are in the range 2.349 (1)–2.487 (1) Å, with an average value of 2.42 (7) Å, which is consistent with the value of 2.38 (7) Å observed<sup>12</sup> in other structures.

There is extensive hydrogen bonding in the structure, involving both the coordinated and the uncoordinated water molecules; the metrical parameters associated with the hydrogen bonding are

**Table V.** Coordination Geometries in Calcium Complexes of Malonate and Substituted Malonate Ions

complex	coordn no.	coordn mode	Ca–O, Å	ref
$[\text{Ca}(\text{mal})(\text{OH}_2)_2]^a$	8	unidentate (2)	2.41 (2)	14
			2.395 (1)	13
		bidentate (2)	2.411 (1)	15
			2.54 (2)	14
			2.528 (6)	13
$[\text{Ca}(\text{mal})(\text{OH}_2)_2]^b$	7	unidentate (3)	2.42 (10)	16
$[\text{Ca}(\text{memal})]^c$	7	malonate (1)	2.47 (15)	16
		unidentate (2)	2.34 (4)	9
$[\text{Ca}(\text{memal})]^c$	7	bidentate (1)	2.52 (6)	9
		malonate (1)	2.374 (17)	9
		unidentate (2)	2.355 (6)	9
$[\text{Ca}(\text{etmal})]$	8	bidentate (2)	2.53 (4)	9
		unidentate (4)	2.45 (8)	8
$[\text{Ca}(\text{bzmalH})_2]$	7	bidentate (1)	2.501 (15)	8
		malonate (1)	2.38 (6)	8
		malonate (1)	2.86 (12)	10
$[\text{Ca}(\text{mal})(\text{OH}_2)_2] \cdot 2\text{H}_2\text{O}$	8	unidentate (5)	2.95 (8)	10
		unidentate (4)	2.42 (7)	d
		bidentate (1)	2.54 (3)	d

<sup>a</sup>Solution-grown form. <sup>b</sup>Gel-grown form. <sup>c</sup>There are two crystallographically independent calcium ions in this structure. <sup>d</sup>This work.

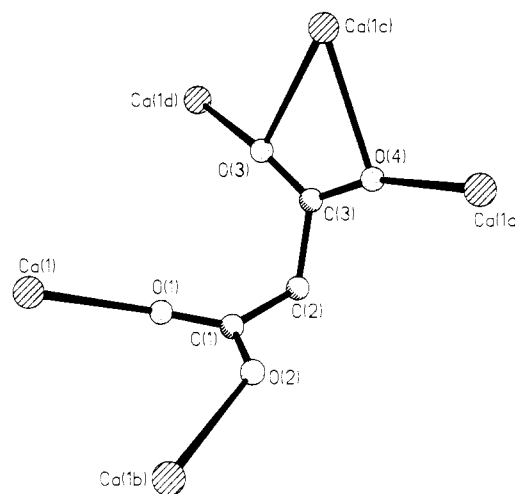


**Figure 3.** View of the bonding of a single malonate dianion in the crystals of  $[\text{Ca}(\text{mal})(\text{OH}_2)_2] \cdot 2\text{H}_2\text{O}$ , showing the five different calcium ions to which the malonate dianion is bonded. Symmetry operations are as in Table IV.

listed in Table S2 (supplementary material). There are eight possible donors in the structure (two hydrogen atoms on each of four water molecules), and all eight participate in hydrogen bonding. Coordinated water molecule O(5W) forms hydrogen bonds to carboxylate oxygen atoms O(1) and O(2) of two different malonate moieties, linking the structure in a chainlike fashion; atom O(1) also accepts a hydrogen bond from the uncoordinated water molecule O(8W). All other hydrogen bonds in the structure involve interactions between the various water molecules, so that the uncoordinated water molecules [O(7W) and O(8W)] each participate in four hydrogen bonds, two as donor and two as acceptor. Coordinated water molecule O(6W) acts as acceptor only in one case, its other electron pair being involved in the bond to calcium, but molecule O(5W) does not act as an acceptor.

The binding of any single malonate ion is shown in Figure 3. As is evident from the figure, each malonate ion binds to five different calcium ions. Each oxygen atom is involved in one unidentate bond, and in addition atoms O(3) and O(4) form the bidentate interaction. The geometry of the malonate ion is similar to that in the other calcium complexes.<sup>13–16</sup> It is normal in malonate ions for the two carboxyl groups to be nearly orthogonal;<sup>10</sup> in the present case, the dihedral angle between the planes O(1)–C(1)–O(2) and O(3)–C(3)–O(4) is 69.2°.

The present structural analysis provides additional evidence for our contention<sup>8,10,11</sup> that the major reason for the presence of Gla rather than Glu in calcium-binding proteins is the availability in the former of additional carboxylate moieties that can permit the formation of extensive polymeric arrays of the general kinds found in all of these model complexes. The ability of a metal ion to participate in such aggregation is limited by its ability to adopt a wide variety of geometries, since in the protein the environments available to the metals would surely be irregular. The great flexibility of calcium(II), in contrast to the rigid requirement of precise octahedral geometry for magnesium(II), may allow the protein to discriminate between calcium and magnesium, since the formation of complex polymeric arrays involving magnesium is precluded by the geometric constraints of that metal ion.

**Acknowledgment.** This work was supported by the National Science Foundation through Grant No. CHE-8912675.

**Supplementary Material Available:** Tables S1 (anisotropic and isotropic thermal parameters) and S2 (hydrogen-bonding distances and angles) (2 pages); Table S3 (observed and calculated structure amplitudes) (8 pages). Ordering information is given on any current masthead page.

Contribution from Department of Inorganic Chemistry 1,  
Chemical Centre, University of Lund,  
P.O. Box 124, S-221 00 Lund, Sweden

## Li<sub>2</sub>F<sup>+</sup> and Li<sub>2</sub>OH<sup>+</sup> in Molten Alkali-Metal Nitrate

L. Bengtsson, B. Holmberg,\* and S. Ulvenlund

Received October 19, 1989

### Introduction

Polymetal complexes of the type M<sub>m</sub>X<sup>m+</sup> (X = halide or chalcogenide) are known to play an important role in the solution chemistry of certain mixed molten salt systems and concentrated aqueous solutions.<sup>1–6</sup> Ionic molten salt solvents probably enhance the stability of such polymetal species, which until 1988 were thought to be formed preferably between soft acceptor and donor ions. Iodide complexes with the d<sup>10</sup> ions Hg<sup>2+</sup> and Ag<sup>+</sup> are typical examples,<sup>1–3</sup> but we have recently also characterized Tl<sub>2</sub>Br<sup>+</sup> in molten alkali-metal nitrates.<sup>7</sup>

A further extension of the search for polymetal complexes into the d<sup>10s</sup> metal ion chemistry revealed that Pb<sup>2+</sup> forms Pb<sub>2</sub>X<sup>3+</sup> with halide and hydroxide ions in nitrate melts with the overall thermodynamic stability increasing in the X sequence Cl < Br < I ≈ F ≪ OH.<sup>4,5,8</sup> Hence, the hard donors F<sup>-</sup> and OH<sup>-</sup> can give polymetal complexes of equal or even higher stability than analogous species with softer halides. On the other hand, a thorough thermodynamic and X-ray scattering investigation into the Cd(II) chemistry in nitrate-based melts with compositions that were optimized to yield polycadmium halide complexes gave

conclusive evidence for the complete absence of complex species other than CdX<sup>+</sup> (X = F, Cl, Br, or I).<sup>9</sup> A d<sup>10</sup> valence electron configuration is thus neither sufficient nor necessary for polymetal complexation in the melts.

It has been argued that the effects of cation repulsion may severely reduce the tendency to form polymetal species with a high formal positive ionic charge.<sup>10</sup> The absence of e.g. Cd<sub>2</sub>X<sup>3+</sup> species could of course be explained with such arguments. The stability of Pb<sub>2</sub>F<sup>3+</sup> and Pb<sub>2</sub>OH<sup>3+</sup> has been attributed mainly to direct Pb–Pb bonds, the formation of which must energetically compensate for the repulsion.<sup>6,8</sup> Further work along these lines has recently revealed that the s<sup>2</sup>p<sup>6</sup> ions Sr<sup>2+</sup> and Ba<sup>2+</sup> form M<sub>2</sub>F<sup>3+</sup> in nitrate melts.<sup>11</sup> The extent of direct metal–metal interaction in these complexes is indeed unknown, and no straightforward bonding scheme for polymetal complexes seems to be attainable at present. However, the very fact that the alkaline-earth metal ions do yield M<sub>2</sub>F<sup>3+</sup> species makes the corresponding “low-charge” Li<sup>+</sup> systems highly interesting objects of study. A paramount matter of interest is of course to what extent direct Li–Li interactions may be of importance.

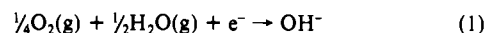
Considering the relevant solution chemistry for Li<sup>+</sup> in water and other molecular solvents, it seems that only one single complex species, viz. LiOH(aq), has been observed.<sup>12–15</sup> No fluoride complexes have been detected.

The aim of the present work is to clarify the possible existence of polyolithium complexes Li<sub>m</sub>X<sup>m–1</sup> in the melts by potentiometric determination of X<sup>-</sup> (X = F or OH) activity changes in systems [(K,Na),Li][X,NO<sub>3</sub>] with the total concentration relation C<sub>Li</sub> > C<sub>X</sub>.

### Experimental Section

**Chemicals.** KNO<sub>3</sub> and NaNO<sub>3</sub> (Merck, p.A.) were dehydrated at 130 °C. KF and LiNO<sub>3</sub> were dried under vacuum at increasing temperatures up to 130 °C. Karl Fischer titrations showed the water content of LiNO<sub>3</sub> to be less than or equal to the detection limit of the method of analysis (≤1.0 × 10<sup>-2</sup> wt %). The chemicals were handled in a glovebox with a dry N<sub>2</sub>(g) atmosphere. The NaOH preparation (EKA, p.A.) contained 95.7 wt % sodium hydroxide, as determined by standard acid–base titration, and water to 100.0 wt %. The O<sub>2</sub>(g) used (Alfax, Oxygene N48; H<sub>2</sub>O < 2 ppm, CO<sub>2</sub> < 0.2 ppm) was passed through Carbosorb (BDH Chemicals, 10–20 mesh) and drying agents before being equilibrated with pure water at 18.6 °C, giving the partial pressures P(H<sub>2</sub>O) = 16 mmHg and P(O<sub>2</sub>) ≈ 744 mmHg.

**Emf Measurements.** The complex formation between Li<sup>+</sup> and F<sup>-</sup> and between Li<sup>+</sup> and OH<sup>-</sup> was studied at temperatures between 240 and 290 °C. Further details about the apparatus, cell construction, and measurement procedures have been thoroughly described previously.<sup>4,8</sup> The fluoride systems were studied with a LaF<sub>3</sub> membrane electrode,<sup>4</sup> and hydroxide activities were measured with a mixed O<sub>2</sub>/H<sub>2</sub>O gas electrode.<sup>8</sup> This [O<sub>2</sub> + H<sub>2</sub>O](g),Pt(s)/OH<sup>-</sup> electrode has been shown to respond reversibly to OH<sup>-</sup> according to the one-electron mechanism



The total concentrations used were  $1.12 \times 10^{-3} \leq C_{\text{OH}}/(\text{mol kg}^{-1}) \leq 1.99 \times 10^{-2}$ ,  $2.50 \times 10^{-3} \leq C_{\text{F}}/(\text{mol kg}^{-1}) \leq 1.04 \times 10^{-2}$ , and  $8.97 \times 10^{-3} \leq C_{\text{Li}}/(\text{mol kg}^{-1}) \leq 1.01$ . The large majority of experimental points had  $C_{\text{Li}}/(\text{mol kg}^{-1}) \leq 0.10$ .

**Raman Spectroscopy.** The furnace and experimental technique were analogous to those reported in earlier publications.<sup>8,9</sup> Only LiNO<sub>3</sub>–(K,Na)NO<sub>3</sub> and LiOH–LiNO<sub>3</sub>–(K,Na)NO<sub>3</sub> melts were investigated, due to the low solubility of LiF.

### Results

**Potentiometric Measurements.** Emf changes are observed when LiNO<sub>3</sub> is added to the (K,Na)(NO<sub>3</sub>,X) melts (X = F, OH). These

- Holmberg, B.; Johansson, G. *Acta Chem. Scand., Ser. A* **1983**, *37*, 367.
- Yamaguchi, T.; Johansson, G.; Holmberg, B.; Maeda, M.; Ohtaki, H. *Acta Chem. Scand., Ser. A* **1984**, *38*, 437.
- Bengtsson, L.; Holmberg, B.; Persson, I.; Iverfeldt, Å. *Inorg. Chim. Acta* **1988**, *146*, 233.
- Bengtsson, L.; Holmberg, B. *J. Chem. Soc., Faraday Trans. 1* **1989**, *85*, 305.
- Bengtsson, L.; Holmberg, B. *J. Chem. Soc., Faraday Trans. 1* **1989**, *85*, 317.
- Bengtsson, L.; Holmberg, B. *J. Chem. Soc., Faraday Trans. 1* **1989**, *85*, 2917.
- Holmberg, B.; Bengtsson, L.; Johansson, R. *J. Chem. Soc., Faraday Trans. 1990*, *86*, 2187.
- Bengtsson, L.; Holmberg, B. *J. Chem. Soc., Faraday Trans. 1990*, *86*, 351.

- Bengtsson, L.; Holmberg, B. *Acta Chem. Scand.* **1990**, *44*, 447.
- Braunstein, J. J. *Electroanal. Chem. Interfacial Electrochem.* **1971**, *33*, 235.
- Bengtsson, L.; Frostemark, F.; Holmberg, B.; Ulvenlund, S. Unpublished results.
- Gimblett, F. G. R.; Monk, C. B. *Trans. Faraday Soc.* **1954**, *50*, 965.
- Spiro, M. *Trans. Faraday Soc.* **1959**, *55*, 1746.
- Ohtaki, H. *Acta Chem. Scand.* **1964**, *18*, 521.
- Masterton, W. L.; Berka, L. H. *J. Phys. Chem.* **1966**, *70*, 1924.